IN VITRO BIOACTIVE FUNCTIONAL OF BIO CERAMICS IN A SIMULATED BODY FLUID

Noriyuki HISAMORI*, Akira NOZUE* Mamoru AIZAWA* and Hiroshi SUEMASU*

* Department of Mechanical Engineering, Sophia University
7-1 Kioi-cho, Chiyoda-ku, Tokyo, 102-8554 Japan
TEL&FAX: +81-3-3238-3318
E-mail : hisamori@me.sophia.ac.jp
http://www.sophia.ac.jp/

ABSTRACT

Apatite ceramics and A-W glass ceramics matrix bonds to living bone through an apatite layer that is formed on its surface in the body. It has been confirmed by SEM observation, thin film X-ray diffraction and FT-IR reflection spectroscopy that the apatite layer can be reproduced on the surface of the hydroxyapatite ceramics and A-W glass ceramics even in an a cellular simulated body fluid with ion concentrations nearly equal to those of human blood plasma. In the present study, structures of bioactive hydroxyapatite ceramics, A-W glass ceramics and the apatite layer formed on its surface in the simulated body fluid were observed under an Atomic Force Microscope (AFM). The apatite layer formed on the substrate apatite ceramics or A-W glass ceramic in the simulated body fluid consisted of the fine apatite particle about 2-3 μ m. The apatite particle in the surface layer was in direct contact with those within the apatite ceramics or A-W glass ceramics without intervention of such hydroxyapatite substrate or A-W glass ceramics substrate.

KEY WORDS

Hydroxyapatite, A-W Glass Ceramics, Bioactive, Simulated Body Fluid, Apatite Layer Form, Fracture resistance, microstructure

INTRODUCTION

Biocompatible materials, such as bioactive ceramics and bioactive glass ceramics can be effective in the repair of bone defects during orthopedics surgery. These materials, calcium phosphates, hydroxyapatite ceramics (HA: $Ca_{10}(PO_4)_6(OH)_2$), tricalcium phosphate (TCP: $Ca_3(PO_4)_2$) etc and A-W glass ceramics [1, 2]. These materials have been found by observation to exhibit varying degrees of osteoconductive behavior. The hydroxyapatite ceramics and bioactive glass ceramics was known as a highly bioactive ceramics, and replacements of lost bone [3, 4]. The same types of the apatite layer was also observed on the surface of hydroxyapatite ceramics and A-W glass ceramics, where as it was not observed on the surface of bioinert ceramics. This indicates that the formation of the apatite layer is prerequisite for the chemical bond of apatite ceramics to living bone. However, detailed structure of the formed apatite layer, such as the size, morphology and composition of the apatite crystal, as well as the detailed microstructure of apatite ceramics and A-W glass ceramics itself has not been revealed yet. The purpose of the present study is to investigate these issues by a high resolution and 3d image AFM.

EXPERIMENTAL PROCEDURE

Preparation of Hydroxyapatite

Submicrometer hydroxyapatite powder (HAp-200 ($Ca_{10}(PO_4)_6(OH)_2$) : 0.3～0.5 μ m average grain size: Taihei chemical industrial Co., Ltd.) were used as starting materials for making hydroxyapatite ceramics. The chemical compositions of this powder were shown in Table1. Pressureless sintering was performed at 1375℃ in O_2 atmosphere using the presintered bodies. And also, A-W glass ceramics, which is commercialized by the name of cerabone A-W, was supplied from Nippon Electric Glass Co., Ltd. (Otsu, Japan). The procedure for preparing the glass-ceramics was previously reported [2]. The dimensions of the soaking specimens used in this study are disk plate size ϕ 16mm×3(t)mm were abraded with the 0.1 μ m diamond paste polished, and washed with pure methanol and distilled water in an ultrasonic cleaner.

TABLE 1
Contents except for hydroxyapatite powder (numerical weight 2000).

Factor	Chloride	Sulfate	Heavy metal (Pb)	Fe
Content [ppm]	20 >	50 >	5 >	10 >
Factor	As	Mg	Mn	
Content [ppm]	1 >	50 >	20 >	

Soaking in Simulated Body Fluid

The hydroxyapatite ceramics specimen were soaking in an a cellular simulated body fluid (SBF) with pH and ion concentration nearly equal to those of human blood plasma [5-8], as given in Table 2, to evaluate their surface bioactivities by examining apatite formation on their surface. The SBF was prepared by dissolving reagent-grade NaCl, $NaHCO_3$, KCl, K_2HPO_4, $3H_2O$, $MgCl_2 \cdot 6H_2O$, $CaCl_2$, and Na_2SO_4 into distilled water, and buffered at pH 7.40 with tris (hydrotymethyl) amminomethane ($(CH_2OH)_3CNH_3$) and hydrochloric acid at 37.0℃. Each specimen was soaked in 30ml of SBF at 37.0℃ foe various periods, and them removed form the fluid and washed with methanol.

TABLE 2
Ion concentrations and pH of simulated body fluid (SBF) and those of human blood plasma.

(mEq/L)

	Na^+	K^+	Ca^{2+}	Mg^{2+}	Cl^-	HCO_3^-	HPO_4^{2-}	SO_4^{2-}	other
Sodium chloride	154.0				154.0				
Ringer fluid	130.4	4.0	2.7		109.4				27.7(Lact.)
Simulated Body Fluid	142.0	5.0	2.5	1.5	147.8	4.2	1.0	0.5	100(Tris)
Blood plasma	142.0	5.0	2.5	1.5	103.0	27.0	1.0	0.5	

Lact : Lactic acid

Tris : Tris-hydroxymethyl - amminomethane

Analysis of Specimen with Surface and SBF

Surface structure changes of the specimens due to the subsequent soaking in SBF were examined by thin film X-ray diffraction [9] (TF-XRD: Model Rint 2000, Ri Rigaku, Japan), FT-IR reflection spectroscopy (FT-IR: Model 8200RH, Shimadzu, Japan) and scanning electron microscopy (SEM: Model JEM6100, JEOL, Japan). Changes in element concentration and pH of SBF due to soaking of the specimens were measured by inductively coupled plasma (ICP) atomic emission spectroscope (Model 7000, Shimadzu, Japan) and pH meter (Model PH82, Yokogawa, Japan). Moreover, higher magnification, nanometric, surface damage and apatite layer evolution is required, instead of traditional micron-order damage evolution by using an in-situ atomic force microscope. Nanometric damage was examined with a scanning atomic force microscopy (AFM) (Model SPM-9500J2, Shimadzu, Japan)

Mechanical Test Methods

Fracture resistance measurements were performed at room temperature, the standard disk-shaped compact specimen is a single edge-notched and fatigue crack disk segment loaded in tension. The general proportions of this specimen configuration are shown Figure 1 and Figure 2.

$$K_C = \frac{P}{Bw^{1/2}} \frac{\left(2+\frac{a}{w}\right)\left\{0.76+4.8\frac{a}{w}-11.58\left(\frac{a}{w}\right)^2+11.43\left(\frac{a}{w}\right)^3-4.08\left(\frac{a}{w}\right)^4\right\}}{\left(1-\frac{a}{w}\right)^{3/2}} \quad \cdots\cdots \quad (1)$$

The fracture resistance (*Kc*) was determining by employing tension testing method (ASTM E399-90). *Kc* values were calculated by using the following equation, where *Kc* is fracture resistance [MPa·$m^{1/2}$], *P* is fracture load [kN], *B* is thickness [cm], *a* is crack length [cm] and w is width [cm] generated in the material tested.

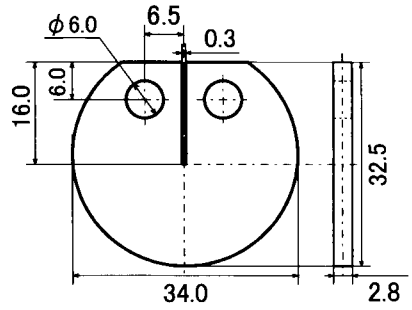

Figure 1 Shape and dimension of specimen

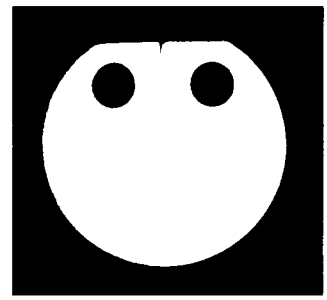

Figure 2 Out looks of Hydroxyapatite CT specimen

RESULTS AND DISCUSSIONS

Bioactive Functional of Apatite Ceramics in a Simulated Body Fluid

Figure 3 shown SEM photographs of sintered surface of apatite ceramics. Figure 4 shown SEM photographs of the cross section of apatite ceramics layer formed that was soaked periods in SBF were (a) 2, (b) 6, and (c) 8weeks. It can be seen from Figure 4 that islandlike substances consisting of particle are formed on all the substrates. Figure 5 shows TF-XRD patterns of the surface of apatite ceramics substrate that were soaked in SBF for 0week and 3weeks. The new XRD peaks appearing after the soaking in SBF are all ascribed to crystalline apatite. Figure 4 show that the islandlike substance formed on the substrate are crystalline apatite and the rate of apatite formation is considerably increased by the soaking periods in SBF for 8weeks. The apatite layer thickness evaluation shown in Figure 6 indicates that the mean thickness increased from 0 μ m to 100 μ m while soaking in SBF for 2,4,6 and 8weeks, respectively.

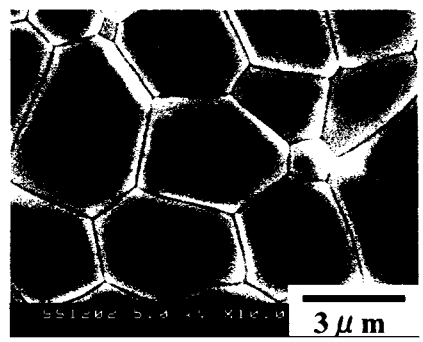

Figure 3 SEM photograph of etched surface of hydroxyapatite ceramic, sintered at 1375℃

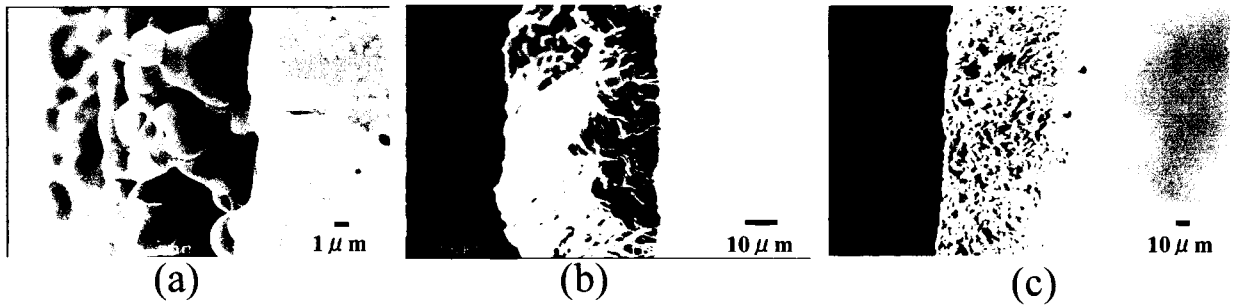

Figure 4 SEM photographs of grown precipitate layer on hydroxyapatite ceramic. ((a) Soaking in SBF for 2weeks, (b) 6weeks, (c) 8weeks)

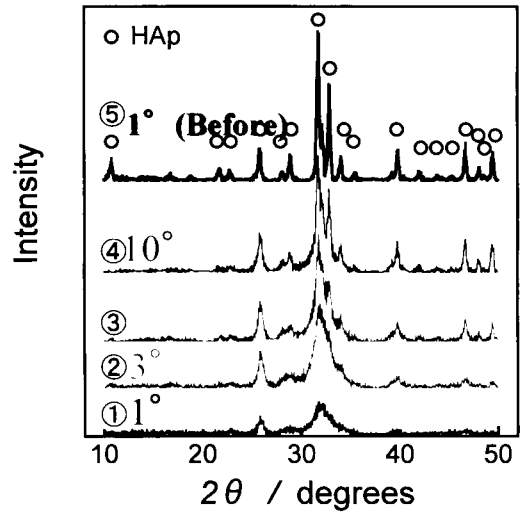

Figure 5 TF-XRD patterns of hydroxyapatite ceramic in SBF (O: hydroxyapatite)

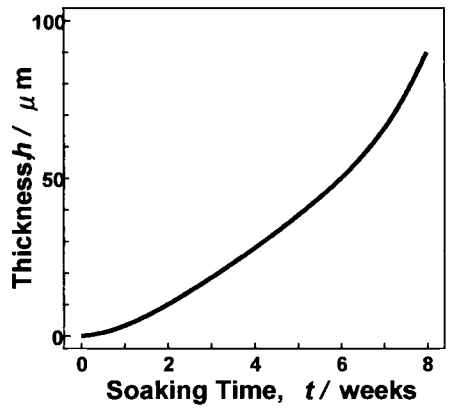

Figure 6 Effects of soaking time on hydroxyapatite particle thickness in SBF

Self-Healing Function of Apatite Ceramics

The room temperature fracture toughness of apatite ceramics, after SBF soaking for from 2 to 8weeks under 37℃, is shown in Figure 7. As a result, corrosion degradation of hydroxyapatite ceramics was preferentially recognized on hydroxyapatite particle after short time immersion into SBF. The general tendency of drastic decrease in fracture toughness was recognized in these materials. In case of materials specimen, most remarkable decrease in fracture toughness after 3weeks immersed into SBF was detected this remarkable degradation in fracture toughness was bought about by the crack propagation behavior of going through into corroded pit (Figure 8). However, the specimens after 4weeks immersion into SBF showed improved fracture toughness compared with those of corroded

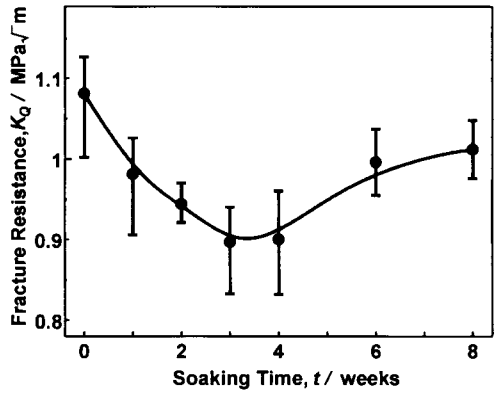

Figure 7. Effects of soaking time on fracture resistance of hydroxyapatite ceramics in SBF

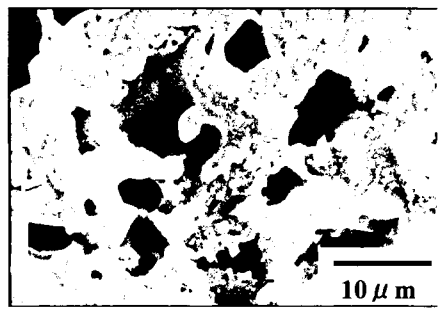

Figure 8 SEM photographs of corroded pits surface of hydroxyapatite ceramics in SBF for 3weeks

hydroxyapatite ceramics (until 3weeks). There improvements in fracture toughness may be brought about through the mechanics was shown to induce the apatite layer formation on it's surface in some areas between 4 and 8weeks by simulated body fluid. The apatite layer formed on the it's hydroxyapatite surface in the SBF consisted of apatite particle about 100 μ m thickness and high interface strength (Figure 6).

In Vitro Bioactive Functional of Apatite Ceramics by In-situ AFM Observation

Through employing AFM analysis, examination of the hydroxyapatite layer formed of the hydroxyapatite ceramics and A-W glass ceramics was conducted. The results are shown in figure 9. Formation of apatite layer was investigated by in-situ AFM observation on the surface of A-W glass ceramics. Effect of apatite layer formed in A-W glass ceramics upon bioactive functional properties were investigated : through examining surface before preconditioned in 37℃ SBF, which were preconditioned in 37℃ SBF solution for 24hr. In case of A-W glass ceramics specimen, most remarkable corrosion pit and grown precipitate was recognized. The specimen of soaking in SBF

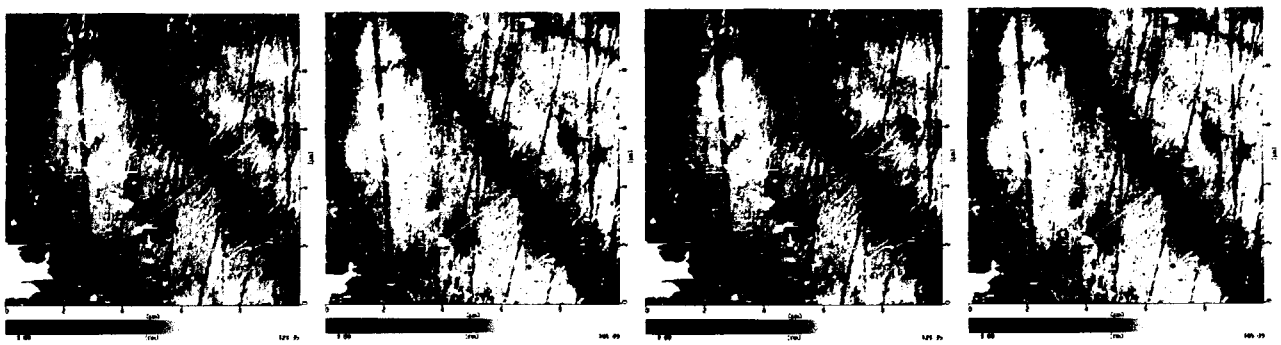

(a) 0min (b) 30min (c) 45min (d) 60min

Figure 9 In-situ visualization of precipitate particle and corrosion products of A-W glass ceramics by AFM in a SBF (1.5) solution, which were preconditioned in 37℃ SBF solution for 24hr.

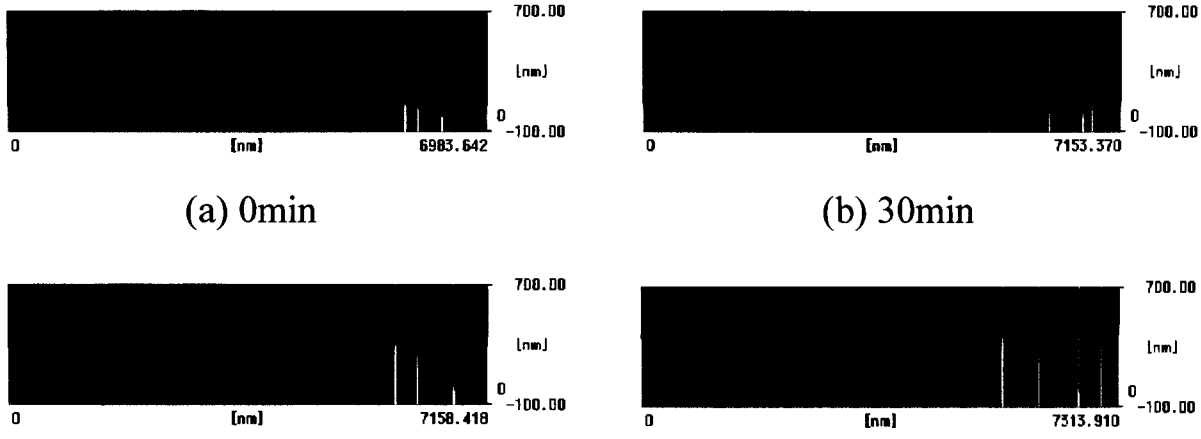

Figure 10 In-situ visualization of precipitate particle and corrosion products of A-W glass ceramics by AFM in a SBF (1.5) solution, which were preconditioned in 37℃ SBF solution for 24hr.

showed the strongest grown precipitate layer and corrosion pit (Figure 10(d)).

SUMMARY

The apatite layer formed on the sintered apatite ceramic in the simulated body fluid consisted of fine needle like apatite particle, which are elongated along C-axis and random oriented. The apatite particles in the surface layer were in direct contact with those within the apatite ceramics substrate without intervention of Ca and P ion. Apatite layer formed in simulated body fluid bought about the fracture resistance changes from corrosion damages to precipitate apatite particle. Nanometreic precipitate apatite particle and corrosion damage is successfully in situ imaged by atomic force microscope.

REFERENCES

1. T.Kokubo, M,Shigematsu, Y.Nagashima, T.Nakamura, T.Yamamuro and S.Higashi, Bull, Inst. Chem., Kyoto Univ., **60**, 260-68 (1982)
2. T.Kokubo, S.Ito, S.Sakka and T.Yamamuro, J.Mater. Sci., **21**, 536-40 (1986)
3. G.Emerwin, Ann.Otil. Rhinol Laryngol. **95**, 76 (1986)
4. J.Wilson, E.douek and K.Rust, Bioceramics, **8**, 235 (1985)
5. C.Ohtsuki, H.Kushitani, T.Kokubo, S.Kotani and T.Yamamuro, J. Biomed. Mater. Res., **25**, 1363-70 (1991)
6. Kokubo, S.Ito, Z.T.Zuang, T.Hayashi, S.Sakka, T.Kitsugi and T.Yamamuro, J. Biomed. Mater. Res., **24**, 331-43 (1990)
7. Y.Ebisawa, T.Kokubo, K.Ohura and and T.Yamamuro, J. Mater. Sic.:Mater Med., **1**, 239-44 (1990)
8. T.Kokubo, Y.Ebisawa, Y.Sugimoto, M.Kiyama, K.Ohura, T.Yamamuro, M.Hiraoka and M.Abe,Terre Haute 213-23 (1992)
9. T.Kitsugi, T.Nakamura, T.Yamamuro, T.Kokubo, M.Shibuya and M.Takagi, J. Biomed. Mater. Res., **21**, 1255-71 (1987)